Hindawi
Advances in Mathematical Physics
Volume 2023, Article ID 6648797, 8 pages
https://doi.org/10.1155/2023/6648797

Research Article

Effects of Soret and Dufour on Unsteady Magneto-Convective Transport through a Vertical Perforated Sheet with Chemical Reaction

Md. Mosharrof Hossain,[1] **Md. Hasanuzzaman**,[2] **A. Rahim Laskar**,[3] **and Ashish Barmon**[2]

[1]*Department of Mathematics, Bangladesh University of Engineering & Technology, Dhaka 1000, Bangladesh*
[2]*Department of Mathematics, Khulna University of Engineering & Technology, Khulna 9203, Bangladesh*
[3]*Department of ICT, Hemayetuddin Degree College, Jhalokati 8400, Bangladesh*

Correspondence should be addressed to Md. Hasanuzzaman; hasanuzzaman@math.kuet.ac.bd

Received 24 July 2023; Revised 25 September 2023; Accepted 14 November 2023; Published 2 December 2023

Academic Editor: P. Areias

An investigation of the effects of Soret and Dufour on an unsteady MHD convective transmission over a vertical porous sheet with chemical reaction was introduced throughout this study. The model that formed nonlinear governing equations is transformed by applying the similarity analysis with the help of the finite difference method. The numerical resolutions of the fluid characteristics like velocity, concentration, and temperature are explained graphically. This research also presented the mass transmission rate, heat transmission rate, and the local skin friction coefficient, which are explained in tabular form. The results give the fluid motion and temperature improvement for growing values of the Dofour effect. Also, the fluid velocity and concentration improve for elevated amounts of the Soret effect. The local skin friction improves by around 66% whereas the mass transmission rate lessens by around 247% with the growing Soret number (0.5–2.0).

1. Introduction

It is common for certain non-Newtonian fluids to flow over a vertical surface in the industrial engineering operations. Non-Newtonian fluids include fluids with specific additives, pulps, molten polymers, animal blood, and fossil fuels, etc. Fluid dynamics experts have already provided a detailed explanation for the movement of these non-Newtonian fluids across the stretched surfaces in both vertical and horizontal positions. The natural convective movement known as the hydromagnetic (MHD) movement has drawn the attention of many academics because of its applications in nuclear reactors, MHD generators, geothermal energy extraction, pumps, plasma studies, and boundary layer flow control. These fields have been examined by numerous scholars, including Hossain [1], Gupta [2], Ahmed et al. [3], Kim [4], and Hasanuzzaman et al. [5]. Because of its importance in engineering science, researchers have an interest in the magnetic field generated by the MHD fluid movement system.

The buoyant characteristics generated by the diffusion of chemical species and heat are often the cause of mass transmission and heat generation. Various transport mechanisms for these fields are noticed in industrial applications as well as in nature. Improvements to several chemical technologies can be made by studying the processes, such as the manufacturing of ceramic, higher oil recovery, polymer production, food processing, and underground energy transportation. Heat and mass transport are very important, because of the consequences of chemical reactions in various hydrometallurgical and chemical technology businesses. Muthuchumaraswamy [6] explored the influences of mass transmission on unstable flow via an accelerating isothermal vertical surface with a chemical reaction. The influences of chemical reactions and radiation on MHD movement over a vertical plate with temperature variation were covered by Rajesh et al. [7]. The significance of the diffusion–thermo and thermal–diffusion characteristics for various fluid motions was examined by Eckert and Drake [8].

Because of its uses in the industry, geosciences, and engineering, such as gas-particle trajectories, hydrology, petrology, foam combustion, and turbine blades, many authors regarded the free convection flows that take place in nature and engineering practices as being quite extensive. When mass and heat transmission inside the flux occur simultaneously, the conducting potential becomes more complex. The energy flux is produced by both temperature and mass gradients. Mass fluxes could also be created by temperature gradients. This is called thermal diffusion or Soret influence. Heat fluxes might also be generated by the concentration gradients. This is called the mass diffusion or Dufour impact. The properties of Soret and Dufour on a time-dependent MHD natural convective transportation onto a vertical sheet in a saturated permeable medium were initially outlined by Postelnicu [9]. Matao et al. [10] looked into the consequences of rotation and Hall current on an unstable MHD natural convection transfer of heat and mass movement passing an extended infinite vertical perforated plate with Soret and Dufour characteristics. Jamir and Konwar [11] looked into the impacts of the applied heat source, viscous dissipation, and Soret and Dufour with radiation absorption. The researchers considered an unsteady MHD mixed convective movement with velocity slip condition across the semi-infinite vertical porous surface. Yasir et al. [12] described how thermal energy is transmitted with thermophoretic particle deposition and Soret–Dufour properties. A recent study by Hasanuzzaman et al. [5] explored the consequences of thermal diffusion and Dufour on time-dependent MHD-free convective transport over a vertical perforated sheet. By taking into account internal heat generation and chemical reactions involving thermal radiation, respectively, Hasanuzzaman et al. [13] expanded on the research conducted by Hasanuzzaman et al. [5]. The impact of a chemical reaction on the time-dependent mass transfer and heat transfer flow of a vertical perforated sheet was clarified by Hossain et al. [14].

The main goal of this investigation is to observe the consequences of Soret and Dufour's properties on time-dependent MHD convective transportation across a vertical perforated sheet. The key contribution of this research is correspondingly prolonged by taking the Soret and Dufour effects through the shooting technique which has not been examined yet. By using the shooting technique with MATLAB software, the numerical solution for dimensionless equations like temperature, concentration, and velocity equations are explained graphically. The local skin friction, heat transmission rate, and mass transmission rate are also included in the tabular presentations.

2. Governing Equations with Model

An unstable 2D hydromagnetic convective boundary layer fluid movement of electrically conducting and incompressible viscous fluid flow past a vertical permeable plate embedded in a porous medium is assumed. The direction of the plate has been fixed along the x-axis. The vertical porous plate runs parallel to free-stream velocity. The vertical porous sheet and y-direction are perpendicular. Along the flow, a transverse magnetic field B_0 is applied uniformly. T_w represents the fluid temperature while C_w indicates the concentration at the wall. The permeable plate begins to forcefully move across its surface at a speed U_0 for $t > 0$. We consider the permeable plate to be infinite. So, $\frac{\partial u}{\partial x} \longrightarrow 0$ as $x \longrightarrow 0$. For this reason, the fluid velocity is $\vec{q} = u(y,t)\vec{i} + v(y,t)\vec{j}$. According to the Boussinesq approximation, the fluid density is uniform in the whole simulation. The coordinate system along with flow configuration is presented in Figure 1.

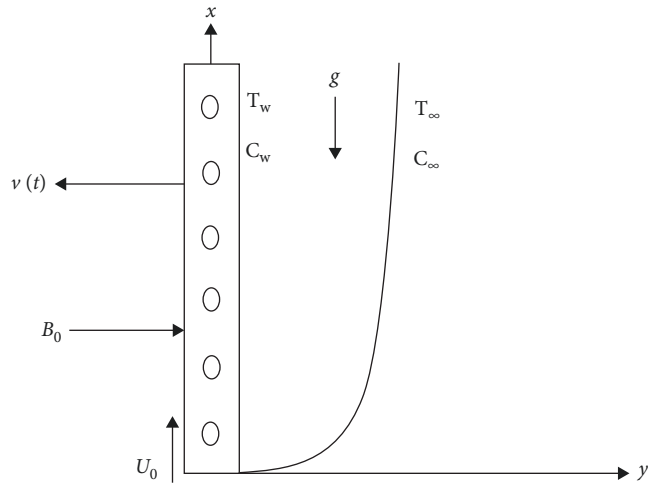

Figure 1: Coordinate system along with physical model.

The governing equations using the Boussinesq approximation [5] are as follows:

$$\frac{\partial v}{\partial y} = 0, \tag{1}$$

$$\frac{\partial u}{\partial t} + v\frac{\partial u}{\partial y} = \upsilon\frac{\partial^2 u}{\partial y^2} + g\beta(T - T_\infty) + g\beta^*(C - C_\infty) - \frac{\sigma' B_0^2}{\rho}u, \tag{2}$$

$$\frac{\partial T}{\partial t} + v\frac{\partial T}{\partial y} = \frac{k}{\rho C_p}\frac{\partial^2 T}{\partial y^2} + \frac{D_m k_T}{C_s C_p}\frac{\partial^2 C}{\partial y^2}, \tag{3}$$

$$\frac{\partial C}{\partial t} + v\frac{\partial C}{\partial y} = \frac{D_m k_T}{T_m}\frac{\partial^2 T}{\partial y^2} + D_m\frac{\partial^2 C}{\partial y^2} - K^*(C - C_\infty). \tag{4}$$

The related boundary conditions are as follows:

$$u = U_0(t), T = T_w, v = v(t), C = C_w \text{ at } y = 0, \tag{5}$$

$$u = 0, T \longrightarrow T_\infty, v = 0, C \longrightarrow C_\infty \text{asy} \longrightarrow, \tag{6}$$

where u and v, respectively, indicate the components of velocity across the x- and y-axes, g is the gravitational acceleration, ρ is the fluid density, thermal conductivity is k, T is the fluid temperature, C is fluid concentration, T_w is the wall temperature, C_w is the wall concentration, C_∞ is fluid concentration in the free stream, T_m is the fluid mean temperature, thermal diffusion ratio is k_T, K^* is the chemical reaction

rate of spices concentration, T_∞ is the fluid temperature in the free stream, mass diffusivity coefficient is D_m, and υ is the kinematic viscosity.

The similarity parameter representing the unsteady length scale (σ) is as follows:

$$\sigma = \sigma(t). \tag{7}$$

The following has been imposed concerning σ as the resolution of the continuity Equation (1)-

$$v = -v_0 \frac{\upsilon}{\sigma}. \tag{8}$$

Here v_0 is the nondimensional normal velocity at the sheet. The conditions $v_0 < 0$ and $v_0 > 0$ signify the injection and suction, respectively.

We consider the similarity variables as follows:

$$\eta = \frac{y}{\sigma}, f(\eta) = \frac{u}{U_0}, \phi(\eta) = \frac{C - C_\infty}{C_w - C_\infty}, \theta(\eta) = \frac{T - T_\infty}{T_w - T_\infty}. \tag{9}$$

The Equations (1)–(4) are changed into the dimensionless couple ODEs by considering the previously mentioned Equations (7)–(9) as follows:

$$f'(\eta) + 2\xi f'(\eta) + Gr\theta(\eta) + Gm\phi(\eta) - Mf(\eta) - \frac{1}{Da} f(\eta) = 0, \tag{10}$$

$$\theta''(\eta) + Pr\left\{Df\phi''(\eta) + 2\xi\theta'(\eta)\right\} = 0, \tag{11}$$

$$\phi''(\eta) + Sh\{2\xi\phi'(\eta) + Sr\theta''(\eta) - Kr\phi(\eta)\} = 0. \tag{12}$$

We have the modified boundary conditions as follows:

$$f(\eta) = 1, \phi(\eta) = 1, \theta(\eta) = 1 \text{ at } \eta = 0, \tag{13}$$

$$f(\eta) = 0, \phi(\eta) = 0, \theta(\eta) = 0 \text{ as } \eta \longrightarrow \infty, \tag{14}$$

where Schmidt number is $Sc = \frac{\upsilon}{D_m}$, $Gr = \frac{g\beta(T_w - T_\infty)\sigma^2}{U_0\upsilon}$ is local Grashof number, Prandtl number is $Pr = \frac{\rho\upsilon C_p}{k}$, $Kr = \frac{K^*\sigma^2}{\upsilon}$ is chemical reaction parameter, $M = \frac{\sigma' B_0^2 \sigma^2}{\rho\upsilon}$ is magnetic force parameter, $Df = \frac{D_m k_T (C_w - C_\infty)}{C_s C_p \upsilon (T_w - T_\infty)}$ is Dufour number, Soret number is $Sr = \frac{D_m k_T (T_w - T_\infty)}{\upsilon T_m (C_w - C_\infty)}$, $Gm = \frac{g\beta^*(C_w - C_\infty)\sigma^2}{U_0\upsilon}$ is modified local Grashof number, and $\xi = \eta + \frac{v_0}{2}$.

The Nusselt number (Nu), Sherwood number (Sh), and the shear stress (τ) represent the flow parameters which can be expressed as follows:

$$Nu \propto -\theta'(0), Sh \propto -\phi'(0), \tau \propto f'(0). \tag{15}$$

3. Numerical Solution

The main target is to utilize the finite difference methods (FDM) to find the solution of the ODEs (10)–(12) including the boundary conditions (13) and (14) in this research. This method has proven to be accurate and effective in resolving a variety of problems [15, 16]. The solution domain space is discretized in the FMD.

We will apply grid size $\Delta\eta = h > 0$ in η-axis, $\Delta\eta = \frac{1}{N}$, with $\eta_i = ih$ where $i = 0, 1, \ldots, N$. Let $f_i = f(\eta_i)$, $\theta_i = \theta(\eta_i)$, and $\phi_i = \phi(\eta_i)$.

At the i^{th} node, we consider F_i, Θ_i, and Φ_i to be the numerical values of $f, \theta,$ and ϕ, respectively. Therefore, we consider:

$$f'|_i = \frac{f_{i+1} - f_{i-1}}{2h}, \theta'|_i = \frac{\theta_{i+1} - \theta_{i-1}}{2h}, \phi'|_i = \frac{\phi_{i+1} - \phi_{i-1}}{2h}, \tag{16}$$

$$f''|_i = \frac{f_{i+1} - 2f_i + f_{i-1}}{h^2}, \theta''|_i = \frac{\theta_{i+1} - 2\theta_i + \theta_{i-1}}{h^2}, \phi''|_i = \frac{\phi_{i+1} - 2\phi_i + \phi_{i-1}}{h^2}. \tag{17}$$

The system of ODES Equations (10)–(12) is discretized by applying FDM in space which is called the main step. To do this we put Equations (16) and (17) into (10)–(12) and neglect the truncation errors. So, taking $i = 0, 1, \ldots, N$, the resulting algebraic equations are as follows:

$$F_{i+1} - 2F_i + F_{i-1} + \xi h(F_{i+1} - F_{i-1}) + Gr\Theta_i + Gm\Phi_i - Mh^2 F_i = 0, \tag{18}$$

$$\Theta_{i+1} - 2\Theta_i + \Theta_{i-1} + Pr[\xi h(\Theta_{i+1} - \Theta_{i-1}) + Df(\Phi_{i+1} - 2\Phi_i + \Phi_{i-1})] = 0, \tag{19}$$

$$\Phi_{i+1} - 2\Phi_i + \Phi_{i-1} + Sc[\xi h(\Phi_{i+1} - \Phi_{i-1}) + Sr(\Theta_{i+1} - 2\Theta_i + \Theta_{i-1}) - Kr\Phi_i] = 0. \tag{20}$$

Also, the boundary conditions are as follows:

$$F_0 = 1, \Theta_0 = 1, \Phi_0 = 1, F_N = 0, \Theta_N = 0, \Phi_N = 0. \tag{21}$$

The Equations from (18) to (20) with the boundary conditions Equation (21) represent a nonlinear system of algebraic equations in $F_i, \Theta_i,$ and Φ_i. The Newton iteration method will be applied in our calculation using MATLAB software considering an appropriate initial resolution.

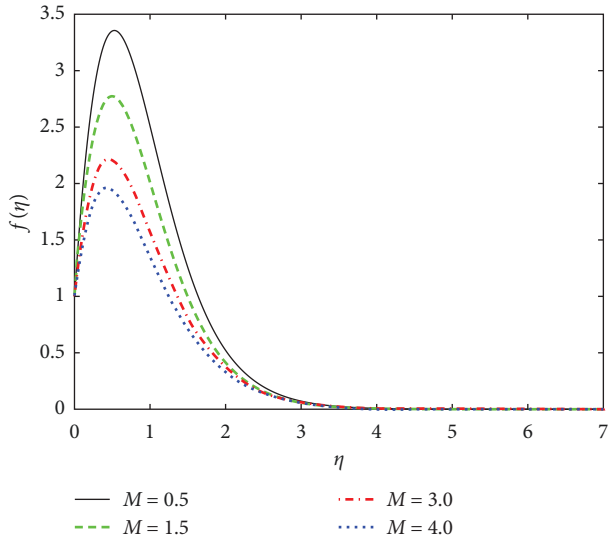

Figure 2: Velocity profile for M.

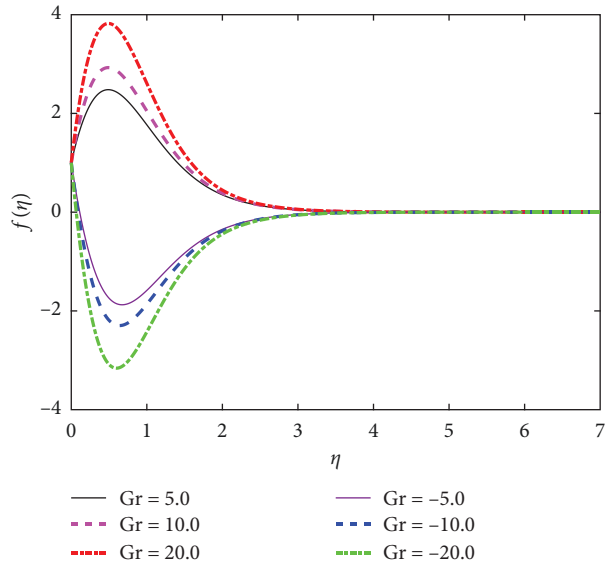

Figure 3: Velocity profile for Gr.

4. Findings and Discussions

A numerical investigation of the unstable free MHD convective transference past a vertical perforated plate with chemical reaction consequences was carried out throughout the study. The Shooting technique was applied to evaluate the numerical solutions of the ODEs Equations (10)–(12). Figures 2–11 demonstrate the fields of fluid temperature, velocity, and concentration for individual quantities of the dimensionless numbers/parameters. We have considered $Sc = 0.22$, $M = 0.5$, $Gr = Gm = 10.0$, $Df = 0.5$, $Sr = 2.0$, $Pr = 0.71$, and $Kr = 0.5$ unless all of the figures specifically state otherwise.

Figure 2 depictures the velocity field for a range of magnetic parameters (M). As the amount of M grows, Figure 2 illustrates how the fluid speed declines. A resistive force known as the Lorentz force is produced by an increase in the magnitude of the magnetic parameter. The fluid velocity is obstructed by this Lorentz force, which lowers the fluid speed. Thus, as the amount of M rises, a physical phenomenon takes place where the velocity distribution drops.

Figure 3 demonstrates the velocity field for several amounts of local Grashof number (Gr). As the amount of Gr goes up, Figure 3 demonstrates how the fluid accelerates. Physically, a rise in Gr leads to the decline of drag force, and hence the velocity fields upgrade in the boundary layer. A symmetrical structure is produced from the velocity field for both positive and negative amounts of Gr. The system is heating for $Gr > 0$.

The consequences of the Dufour number (Df) on velocity and temperature profiles are disclosed in Figures 4 and 5. The Dufour number is the ratio of thermal diffusion (k_T) and kinematic viscosity (υ). The mathematical formula of the Dufour number is $Df = \frac{D_m k_T (C_w - C_\infty)}{C_s C_p \upsilon (T_w - T_\infty)}$. From Figure 4, it can be concluded that the kinematic viscosity lessens for moving amounts of Df. It means that the fluid particles freely move in the computational domain. Because of this, the fluid

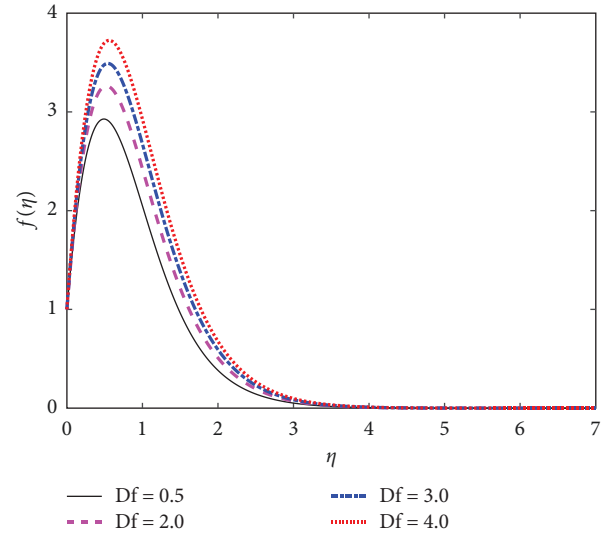

Figure 4: Velocity profile for Df.

velocity improves for growing amounts of Df. We can conclude from Figure 5 that with uplifting amounts of Df, the thermal diffusion improves. It means that the heat transmission rate reduces for rising amounts of Df. It means that rising quantities of Df cause to reduction in the heat transference rate. Because of this, the fluid temperature advances for growing quantities of Df. The effect of the potent Dufour impacts is significantly accelerated by the thermal boundary layer thickness.

Figures 6 and 7 present the concentration and velocity distributions for several quantities of Soret number (Sr). The mathematical formula for Sr is given by $Sr = \frac{D_m k_T (T_w - T_\infty)}{\upsilon T_m (C_w - C_\infty)}$. So, Sr expresses the ratio of mass diffusivity coefficient (D_m) to kinematic viscosity (υ). The kinematic viscosity (υ) has an inverse relationship with the Soret number. Observing Figure 6, we can conclude that the kinematic viscosity lessens

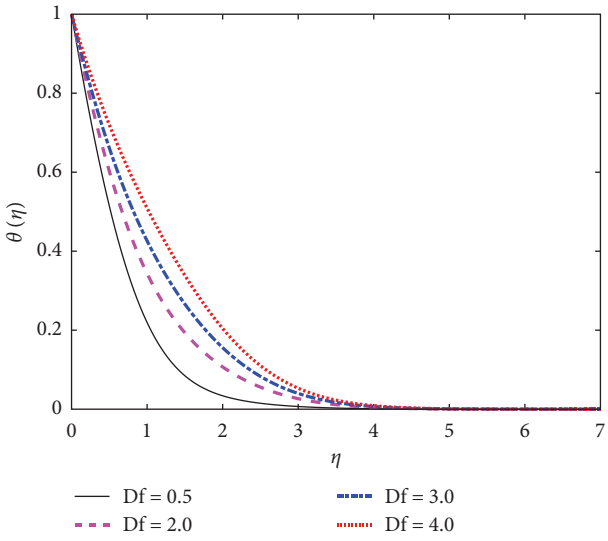

Figure 5: Temperature profile for Df.

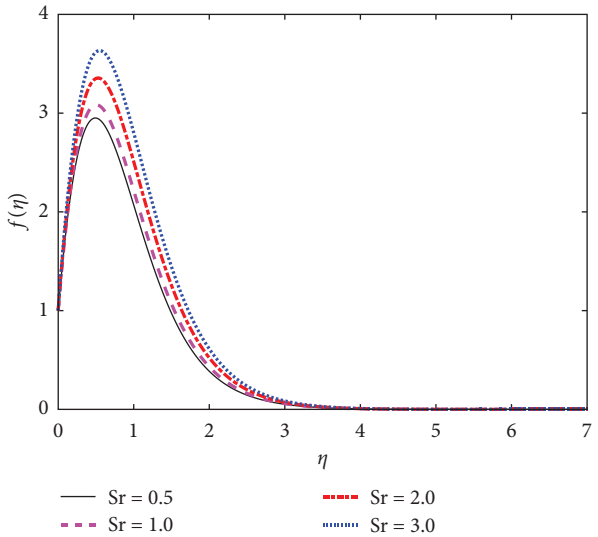

Figure 6: Velocity profile for Sr.

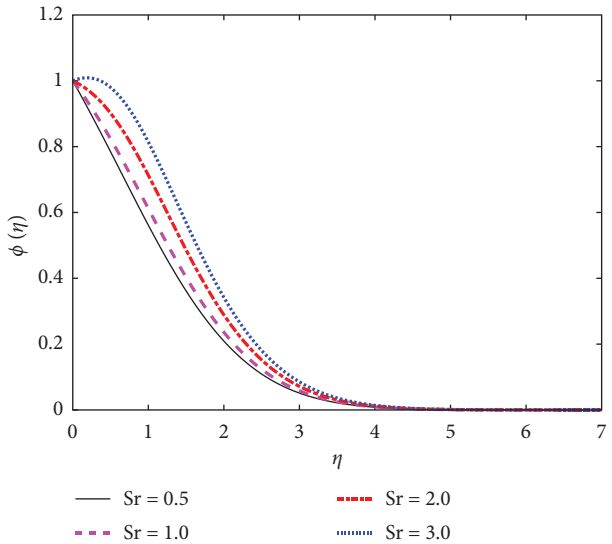

Figure 7: Concentration profile for Sr.

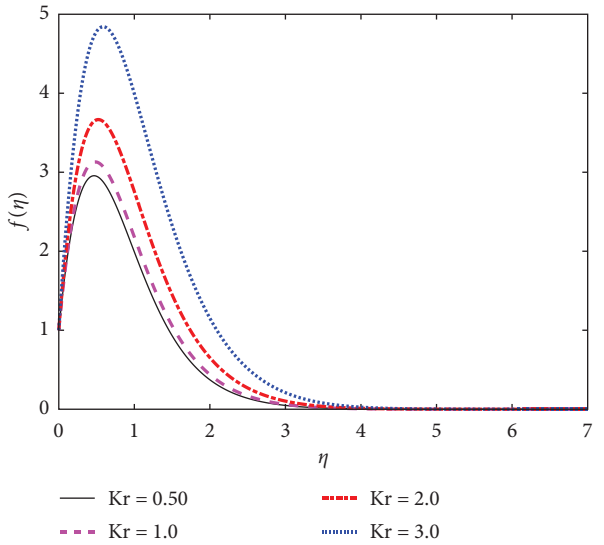

Figure 8: Velocity profile for Kr.

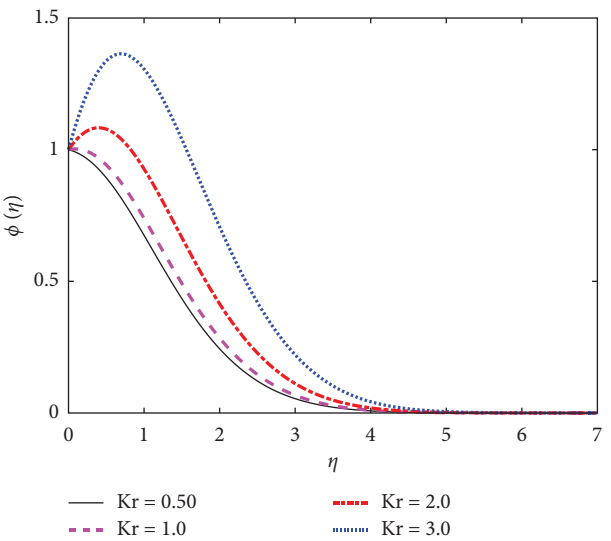

Figure 9: Concentration profile for Kr.

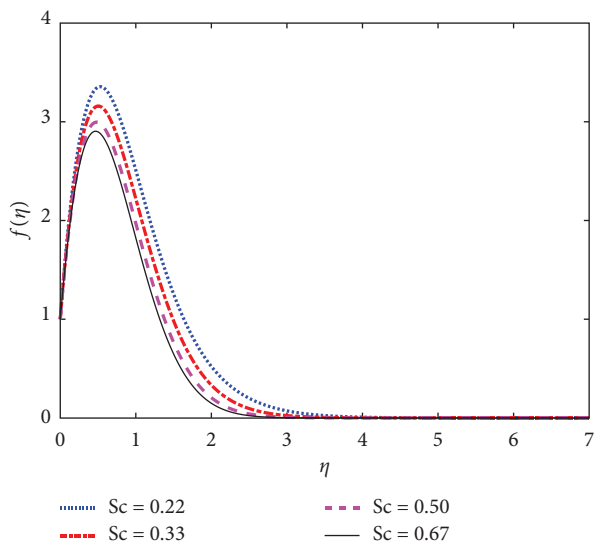

Figure 10: Velocity profile for Sc.

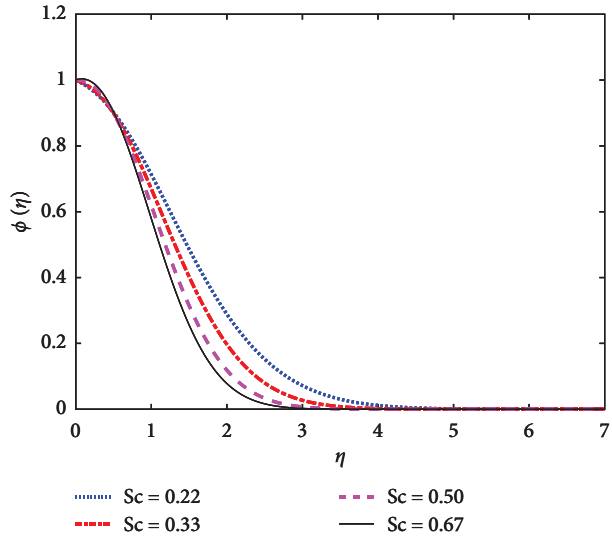

Figure 11: Concentration profile for Sc.

Table 1: Influence of the chemical reaction parameter (Kr) on the parameters $-\theta'(0)$, $f'(0)$, and $-\phi'(0)$.

Kr	$-\theta'(0)$	$f'(0)$	$-\phi'(0)$
0.5	5.51391564856181	8.17165072546812	5.65217488955874
1.0	5.51391564856181	8.81252207805749	6.03222857911580
2.0	5.51391564856181	10.7272329139029	7.05364696931014
3.0	5.51391564856181	14.8081257483379	8.92927321862237

for improving values of Sr. Accordingly, improving quantities of Sr results in less friction force. This enables the fluid to move without restriction within the simulation domain. Hence the fluid velocity enhances for improving amounts of Sr. Also, the mass diffusivity coefficient (D_m) has a proportional relationship with the Soret number. Figure 7 states that the mass diffusivity coefficient upsurges for improving amounts of Sr. The Soret effect develops when there is a differential between light and heavy molecules owing to the temperature gradient, then the mass transfer rate reduces. Hence, the fluid concentration improves for mounting quantities of Sr. Consequently, the concentration distribution is remarkably improved due to uprising amounts of Sr. To raise the concentration boundary layer thickness, this result is crucial.

The concentration and velocity fields are affected by the chemical reaction parameter (Kr), according to Figures 8 and 9. Figure 8 reveals that for higher levels of Kr, the fluid motion improved substantially. The figure demonstrates how significantly the concentration distribution is impacted by Kr. Physically, the interfacial mass transfer rate gets reduced by Kr, which raises the concentration level. Consequently, rising levels of Kr cause the fluid concentration to develop.

Figures 10 and 11 reveal the concentration and velocity fields for several amounts of Schmidt number (Sc). Figure 10 confirms that velocity lessens with an improvement of Sc. Growing amounts of Sc show a reduction in mass diffusivity since Sc is the ratio of kinematic viscosity to mass diffusivity. Moreover, the medium becomes more viscous, which reduces the fluid's movement. We conclude from Figure 11 that the concentration border layer becomes thinner for growing levels of Sc. This causes the concentration patterns to decline. Physically, when the amount of Sc is turned up, the molecule diffusivity reduces. Therefore, the species concentration level rises for a small quantity of Sc and drops for larger levels of Sc. In addition, we note that the concentration field initially develops very near the wall ($0.0 \leq \eta \leq 0.5$), then exhibits the opposite pattern as previously described, and ultimately approaches asymptotically to zero as $\eta \longrightarrow 7$.

5. Mass Transfer Rate, Local Skin Friction Coefficient, and Heat Transfer Rate

The authors are very much interested in presenting the mass transfer rate ($\phi'(0)$), heat transfer rate ($\theta'(0)$), and local skin friction coefficient ($f'(0)$) in the tabular formations. The roles of numerous amounts of the dimensionless parameters/numbers such as Prandtl number (Pr), chemical reaction parameter (Kr), Schmidt number (Sc), and Soret number (Sr) on $f'(0)$, $\theta'(0)$, and $\phi'(0)$ have been explained in Tables 1–4.

Tables 1–4, respectively, reveal the effects of the chemical reaction parameter (Kr), the Prandtl number (Pr), the Schmidt number (Sc), and the Soret number (Sr) on the local skin friction coefficient ($f'(0)$), heat transfer rate ($\theta'(0)$) and mass transfer rate ($\phi'(0)$). It is found from these above

Table 2: Effects of prandtl number (Pr) on the parameters $-\theta'(0)$, $f'(0)$, and $-\phi'(0)$.

Pr	$-\theta'(0)$	$f'(0)$	$-\phi'(0)$
0.71	1.18771638573335	8.85864448239019	5.65217488955874
1.0	1.46476825328160	8.65656548497696	5.65217488955874
7.0	5.51391564856181	8.17165072546812	5.65217488955874

Table 3: The impacts of Schmidt number (Sc) on the parameters $-\theta'(0), f'(0)$, and $-\phi'(0)$.

Sc	$-\theta'(0)$	$f'(0)$	$-\phi'(0)$
0.22	1.18771638498749	10.0746012675587	0.108384307585017
0.33	1.18771638885577	9.62366576116527	0.069720416725401
0.50	1.18771638572732	9.24679191460255	0.002505812448533
0.67	1.18771638574022	9.03351205400936	0.081416805495035

Table 4: The impacts of Soret number (Sr) on the parameters $-\theta'(0)f'(0)$, and $-\phi'(0)$.

Sr	$-\theta'(0)$	$f'(0)$	$-\phi'(0)$
0.5	5.51391564856181	4.90590851190151	0.671996141325176
1.0	5.51391564856181	5.99448920651541	2.33205569339520
2.0	5.51391564856181	8.17165072546812	5.65217488955874

Tables that the values of $f'(0)$ enhance for higher values of Kr and Sr. On the other hand, with an increase in Pr, and Sc the values of $f'(0)$ diminish. The values of $f'(0)$ increase by about 31%, and 66% due to improving values of Kr from 0.5 to 2.0, and Sr from 0.5 to 2.0, respectively. Besides, the value of $f'(0)$ reduces by about 8%, and 10% for higher values of Pr from 0.71 to 7.0 and Sc from 0.22 to 0.67, respectively. The heat transfer rate is enhanced with upward values of Pr. The values of $\theta'(0)$ improve by about 23% due to uplifting values of Pr from 0.71 to 1.0. For this reason, the fluid temperature improves for higher values of Pr. The values of $\phi'(0)$ enhance by about 58%, and 247% due to growing values of Kr from 0.5 to 2.0, and Sr from 0.5 to 2.0, respectively. Also, the mass transfer rate decays by about 25% for higher values of Sc from 0.22 to 0.67.

6. Conclusions

We analyzed the effects of the Soret and Dufour on unstable MHD convective transmission over a vertical porous sheet in the presence of the chemical reaction. The following remarks can be concluded as:

(i) The fluid velocity upgrades for improving amounts of Gr, Df, Sr, and Kr, but declines with growing amounts of magnetic field.

(ii) For higher values of Sr and Kr, the species concentration is enhanced significantly.

(iii) The fluid temperature advances for higher values of Df.

(iv) The velocity lessens with an improvement of Sc.

(v) The flow parameters $f'(0)$ and $\phi'(0)$ are enhanced by about 31% % and 58% for higher values of Kr from 0.5 to 2.0.

(vi) Both $f'(0)$ and $\phi'(0)$ declined by about 10% and 25%, respectively, for higher amounts of Sc (0.22–0.67).

(vii) Both $f'(0)$ and $\phi'(0)$ enhanced by about 66% % and 247%, respectively, for higher amounts of Sr (0.5–2.0).

Nomenclature

MHD: Hydromagnetic
$f'(0)$: Local skin friction coefficient
C: Fluid concentration
T_w: Wall temperature
u: Velocity component in the x-axis
v(t): Suction velocity
υ: Kinematic viscosity
C_w: Wall concentration
T_m: Mean fluid temperature
σ: Similarity parameter
D_m: Mass diffusivity coefficient
$\theta(\eta)$: Non-dimensional temperature
Gr: Local Grashof number
v: Velocity component in the y-axis,
Df: Dafour number
Sc: Schmidt number
τ: Shear stress
S_h: Sherwood number

k_T: Thermal diffusion ratio
k: Thermal conductivity
C_∞: Free stream concentration
$f(\eta)$: Non-dimensional velocity
T: Fluid temperature
B_0: Uniform magnetic field
ρ: Fluid density
$U_0(t)$: Uniform surface velocity
g: Acceleration due to gravity
T_∞: Free stream temperature
Gm: Modified local Grashof number
v_0: Suction and blowing
Pr: Prandtl number
Kr: Chemical reaction parameter
$\theta'(0)$: Heat transfer rate
$\phi(\eta)$: Nondimensional concentration
M: Magnetic force parameter
$\phi'(0)$: Mass transfer rate
N_u: Nusselt number
Sr: Soret number
C_s: Concentration susceptibility
C_p: Specific heat at constant pressure

Data Availability

No data were used for the research described in the article.

Conflicts of Interest

The authors declare that they have no conflicts of interest.

References

[1] M. A. Hossain, "Effect of hall current on unsteady hydromagnetic free convection flow near an infinite vertical porous plate," *Journal of the Physical Society of Japan*, vol. 55, no. 7, pp. 2183–2190, 1986.

[2] A. S. Gupta, "Laminar free convection flow of an electrically conducting fluid from a vertical plate with uniform surface heat flux and variable wall temperature in the presence of a magnetic field," *Zeitschrift für Angewandte Mathematik und Physik ZAMP*, vol. 13, no. 4, pp. 324–333, 1962.

[3] N. Ahmed, H. K. Sarmah, and D. Kalita, "Thermal diffusion effect on a three-dimensional MHD free convection with mass transfer flow from a porous vertical plate," *Latin American Applied Research*, vol. 41, no. 2, pp. 165–176, 2011.

[4] Y. J. Kim, "Unsteady MHD convective heat transfer past a semi-infinite vertical porous moving plate with variable suction," *International Journal of Engineering Science*, vol. 38, no. 8, pp. 833–845, 2000.

[5] M. Hasanuzzaman, M. A. K. Azad, and M. M. Hossain, "Effects of Dufour and thermal diffusion on unsteady MHD free convection and mass transfer flow through an infinite vertical permeable sheet," *SN Applied Sciences*, vol. 3, no. 12, p. 882, 2021.

[6] R. Muthuchumaraswamy, "First order chemical reaction on exponentially accelerated isothermal vertical plate with mass diffusion," *Annals Faculty of Engineering*, vol. 7, pp. 47–50, 2009.

[7] V. Rajesh and S. V. K. Varma, "Chemical reaction and radiation effects on MHD flow past an infinite vertical plate with variable temperature," *Far East Journal of Mathematical Sciences*, vol. 32, pp. 87–106, 2009.

[8] E. R. G. Eckert and R. M. Drake, *Analysis of Heat and Mass Transfer*, McGraw-Hill Book Company, New York, 1972.

[9] A. Postelnicu, "Influence of a magnetic field on heat and mass transfer by natural convection from vertical surfaces in porous media considering Soret and Dufour effects," *International Journal of Heat and Mass Transfer*, vol. 47, no. 6-7, pp. 1467–1472, 2004.

[10] P. Matao, B. P. Reddy, and J. Sunzu, "Hall and rotation effects on radiating and reacting MHD Flow past an accelerated permeable plate with Soret and Dufour Effects," *Trends in Sciences*, vol. 19, no. 5, pp. 2879–2879, 2022.

[11] T. Jamir and H. Konwar, "Effects of radiation absorption, soret, and dufour on unsteady MHD mixed convective flow past a vertical permeable plate with slip condition and viscous dissipation," *Journal of Heat and Mass Transfer Research*, vol. 9, no. 2, pp. 155–168, 2022.

[12] M. Yasir, M. Khan, and Z. U. Malik, "Analysis of thermophoretic particle deposition with Soret–Dufour in a flow of fluid exhibit relaxation/retardation times effect," *International Communications in Heat and Mass Transfer*, vol. 141, Article ID 106577, 2023.

[13] M. Hasanuzzaman, S. Sharin, T. Hassan, M. A. Kabir, R. Afroj, and A. Miyara, "Unsteady magneto-convective heat-mass transport passing in a vertical permeable sheet with internal heat generation effect," *Transportation Engineering*, vol. 9, Article ID 100126, 2022.

[14] M. M. Hossain, A. R. Laskar, and M. F. Afroz Bhuiyan, "Effect of chemical reaction on unsteady MHD convective transport passing a vertical porous sheet," *Journal of Engineering Science*, vol. 14, no. 1, pp. 85–93, 2023.

[15] J. C. Ali, E. A. Sameh, and S. A. Abdulkareem, "Melting and radiation effects on mixed convection from a vertical surface embedded in a non-Newtonian fluid saturated non-Darcy porous medium for aiding and opposing eternal flows," *International Journal of Physical Sciences*, vol. 5, no. 7, pp. 1212–1224, 2010.

[16] W. T. Cheng and C. H. Lin, "Unsteady mass transfer in mixed convective heat flow from a vertical plate embedded in a liquid-saturated porous medium with melting effect," *International Communications in Heat and Mass Transfer*, vol. 35, no. 10, pp. 1350–1354, 2008.